Energy Aware Iterative Source Localization for Wireless Sensor Networks

Engin Maşazade, *Student Member, IEEE*, Ruixin Niu, *Member, IEEE*, Pramod K. Varshney, *Fellow, IEEE*, and Mehmet Keskinoz, *Member, IEEE*

***Abstract*—In this paper, the source localization problem in wireless sensor networks is investigated where the location of the source is estimated based on the quantized measurements received from sensors in the field. An energy efficient iterative source localization scheme is proposed where the algorithm begins with a coarse location estimate obtained from measurement data from a set of anchor sensors. Based on the available data at each iteration, the posterior probability density function (pdf) of the source location is approximated using an importance sampling based Monte Carlo method and this information is utilized to activate a number of non-anchor sensors. Two sensor selection metrics namely the mutual information and the posterior Cramér–Rao lower bound (PCRLB) are employed and their performance compared. Further, the approximate posterior pdf of the source location is used to compress the quantized data of each activated sensor using distributed data compression techniques. Simulation results show that with significantly less computation, the PCRLB based iterative sensor selection method achieves similar mean squared error (MSE) performance as compared to the state-of-the-art mutual information based sensor selection method. By selecting only the most informative sensors and compressing their data prior to transmission to the fusion center, the iterative source localization method reduces the communication requirements significantly and thereby results in energy savings.**

***Index Terms*—Distributed source coding, Monte Carlo methods, posterior Cramér–Rao lower bound, source localization, wireless sensor networks.**

I. Introduction

WIRELESS sensor networks (WSNs) are composed of a large number of densely deployed sensor nodes that cooperatively monitor the physical or environmental conditions of an event of interest such as temperature or velocity of an object. WSNs have a wide range of application areas such as battlefield surveillance, environment or health monitoring, and disaster relief operations. In these applications, WSNs are used for a variety of tasks such as detection, recognition, localization and tracking of objects or events of interest. In this paper, we study the source localization problem where the aim is to estimate the coordinates of an energy emitting source (e.g., acoustic source).

In a region of interest (ROI), an accurate estimate of the source location can be obtained by using the energy readings of the sensors [1], [2]. In [1] and [2], maximum likelihood (ML) based approaches have been proposed by using analog and multi-bit (M-bit) sensor measurements respectively at the fusion center. In this work, we assume that each sensor measurement is quantized into M-bits and delivered to the fusion center over an error-free channel. Simultaneous transmission of all sensors' M-bit data to the fusion center introduces some challenges. First of all, the sensors that are far from the source location are not likely to carry much useful information but they still consume energy to transmit information. Secondly, each sensor requires an independent channel for simultaneous data transmission to the fusion center. This assumption imposes a limitation on the number of sensors that the system can support in practice. Therefore, rather than transmitting multi-bit data from all the sensors, we first employ measurements from a relatively few anchor sensors to obtain a coarse location estimate. In the literature, anchor sensors are utilized to find the sensor node locations [3], [4]. In this work, we assume that sensor placements are known *a priori* at the fusion center and try to estimate the source location. Our iterative algorithm starts when the anchor sensors send their multi-bit data to the fusion center. The non-anchor sensors do not transmit their measurements in the initial phase. A few non-anchor sensors are activated at each step of our iterative procedure. Now the problem is to select the set of non-anchor sensors at each iterative step which improve the accuracy of the source location estimate the most. These activated sensors send their multi-bit measurement data to the fusion center to refine the location estimate. Distributed compression of measurement data prior to transmission is also employed at the non-anchor sensors to further reduce the energy consumption. Thus, we achieve significant energy savings in source localization at the cost of tolerating some delay.

The sensor selection problem in sensor networks has been widely studied in the literature. For sensor management, information based measures have been recently proposed as objective functions to choose the sensing action that maximizes the expected gain in information [5]–[12]. In [5], a sensor selection approach has been proposed which chooses the sensors having maximum mutual information with source location based on analog sensor measurements. In [6], authors focus on using the expected change in Shannon entropy when tracking a

Manuscript received October 07, 2009; May 06, 2010; accepted May 07, 2010. Date of publication June 01, 2010; date of current version August 11, 2010. The associate editor coordinating the review of this manuscript and approving it for publication was Prof. Dominic K. C. Ho. This work is supported in part by the ARO Grant W911NF-09-1-0244. The work of M. Keskinoz is supported by TUBITAK under Grant 105E161. This work was presented in part at the IEEE Third International Workshop on Computational Advances in Multi-Sensor Adaptive Processing (CAMSAP), Aruba, December 13–16, 2009.

E. Maşazade and M. Keskinoz are with the Faculty of Engineering and Natural Sciences, Sabanci University, Istanbul, 34956, Turkey (e-mail: enginm@su.sabanciuniv.edu, keskinoz@sabanciuniv.edu).

R. Niu and P. K. Varshney are with the Department of Electrical Engineering and Computer Science, Syracuse University, Syracuse, NY 13244 USA (e-mail: rniu@syr.edu, varshney@syr.edu).

Color versions of one or more of the figures in this paper are available online at http://ieeexplore.ieee.org.

Digital Object Identifier 10.1109/TSP.2010.2051433

single target. In [7], [8], authors have compared several sensor selection approaches involving entropy and relative entropy. Kreucher *et al.* [9], [10] have proposed sensor management schemes that maximize the Rényi divergence between the current target state probability density and the density after a new measurement arrives. In [11], [12], sensors are selected to maximize the mutual information between the sensor measurements and the target state.

The posterior Cramér–Rao lower bound (PCRLB) is a very important tool because it provides a theoretical performance limit for a Bayesian estimator. In [13], Tichavsky *et al.* derived an elegant recursive approach to calculate the sequential PCRLB for a general multi-dimensional discrete-time nonlinear filtering problem. In [14], based on the PCRLB, a sensor deployment approach is developed to achieve better tracking accuracy while at the same time it uses the limited sensor resources more efficiently. Such approaches are extended in [15] to incorporate sensor deployment and motion uncertainties. For single target tracking, a subset of sensors are selected in a bearing-only sensor network to minimize the PCRLB on the estimation error, where the selected sensors transmit analog data [16] or quantized data [17] to the fusion center. Further, the PCRLB based criterion has been employed to manage sensor arrays for multi-target tracking problems [18], [19]. Another related work is reported in [20], where a PCRLB based adaptive radar waveform design method for target tracking has been presented.

Mutual information and PCRLB are actually related to each other. The work presented in [21] shows that asymptotically the lower bound of the mutual information is a function of the Fisher information. However, the complexity to compute mutual information is much higher than that of computing the PCRLB, especially when the number of sensors to be selected, A, is large. If the sensors provide quantized data, we show in this paper that the computational complexity of the mutual information is exponential in A, whereas the complexity of the PCRLB is linear in A. This fact makes the sensor management based on information theoretic measures impractical when A is large.

In this paper, we first extend the mutual information based sensor selection scheme presented in [12] for quantized sensor measurements. Then, we define another metric for sensor selection based on the PCRLB. Note that in [22] the recursive approach presented in [13] is utilized to calculate the PCRLB. In this work, we re-formulate the PCRLB-based sensor selection metric for static source location estimation. We approximate the posterior pdf of the source location using an importance sampling based Monte Carlo method [23] and by using this approximate posterior pdf, a number of non-anchor sensors are selected in an iterative manner. For sensor selection at each iteration, we compare the PCRLB based sensor selection metric with the state-of-the-art mutual information based sensor selection metric in terms of estimation accuracy and computational complexity. Simulation results show that, within a few iterations, the mean squared error of the estimation approaches the PCRLB of a Bayesian estimate based on all the sensor data. Since the fusion center is not likely to request multi-bit data from the non-informative sensors, which are typically far away from the source location, the proposed iterative algorithm is expected to provide large energy savings.

When sensors are densely deployed in a region of interest (ROI), the sensor measurements are likely to be spatially correlated and this correlation can be utilized to compress the quantized measurements of each sensor prior to transmission to further reduce energy consumption [24], [25]. Given the multi-bit data received during previous iterations and the posterior pdf of the source location, the fusion center calculates the conditional entropy of the sensors to be activated during an iteration and it requests a compressed version of sensor's multi-bit data. Simulation results show that for the first few iterations, the uncertainty about the source location is high which implies a high conditional entropy for the sensor to be activated. In such circumstances, data compression does not have much effect and each sensor measurement is sent to the fusion center using almost M-bits. Including new data at each iteration reduces the uncertainty about the source location and the conditional entropy of each activated sensor gets smaller at each iteration. After the most informative sensors about the source location have been selected, the conditional entropy for each activated sensor becomes very small and only a small number of bits are requested by the fusion center. Hence, data compression yields further energy savings.

The rest of the paper is organized as follows. In Section II, we introduce the system model. In Section III, we present the iterative source location estimation algorithm, where we explain the approximation of the posterior pdf of source location using a Monte Carlo method and describe the mutual information and PCRLB based sensor selection methods. In Section IV, we discuss data compression using the distributed source coding approach. In Section V, we compare the two sensor selection schemes in terms of computation time and give numerical examples to show their estimation performance. Also in Section V, we study the tradeoff between estimation performance and communication cost. Finally, Section VI is devoted to our conclusions and discussion of results.

II. System Model

We consider a WSN consisting of N sensors $\{s_k, k = 1, 2, \ldots, N\}$. We assume that a signal (e.g., an acoustic signal) is radiated from a location (x, y) that follows an isotropic power attenuation model. In this paper, we assume that the source is based on flat ground and all the sensors and source have the same height so that a 2-D model is sufficient to formulate the problem. As an example, an acoustic event on the ground can be analyzed using a 2-D scenario as shown in Fig. 1. In this paper, we assume that N sensors are deployed in a grid layout and the WSN uses a parallel architecture where the quantized measurements of each sensor are directly delivered to the fusion center. The assumption of grid layout is not necessary. Source localization based on sensor readings can be performed for an arbitrary network layout if sensor placements are known in advance. The location of each sensor (s_k) is represented by (x_k, y_k). Then, the distance between s_k and the source location (x, y) is $d_k = \sqrt{(x - x_k)^2 + (y - y_k)^2}$. The received source energy a_k^2 at s_k is expressed as [2]

$$a_k^2 = P_0 \left(\frac{d_0}{d_k} \right)^n \tag{1}$$

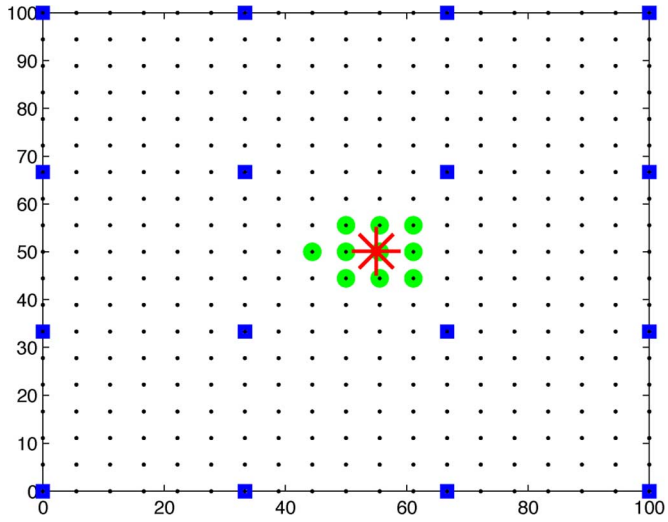

Fig. 1. Wireless Sensor Network Model. Black Points: Sensor Locations; Blue Squares: Anchor Sensors used for initial iteration; Green Circles: Activated Sensors after 10 iterations for the example considered in Section V; Red Star: Source. $A = 1$ sensor is activated per iteration.

where P_0 is the signal power measured at a reference distance d_0 (In this paper, we set $d_0 = 1$ m.), a_k is the received signal amplitude at sensor s_k and n is the signal decay exponent. At each sensor, the received signal amplitude a_k is corrupted by an additive Gaussian noise:

$$r_k = a_k + w_k \tag{2}$$

where r_k is the noisy signal measurement at sensor s_k. Here, we assume that the noise w_k is independent and identically distributed across sensors with Gaussian distribution $\mathcal{N}(0, \sigma^2)$ with $\sigma^2 = 1$.

Let D_k be the M-bit quantized measurement of r_k which takes a discrete value from 0 to $2^M - 1$ where $L = 2^M$ is the number of quantization levels. We assume the same set of quantization thresholds at all the sensors $\boldsymbol{\eta} = [\eta_0, \eta_1, \ldots, \eta_L]^T$ where $\eta_0 = -\infty$ and $\eta_L = \infty$. Then D_k is obtained from r_k as

$$D_k = \begin{cases} 0 & -\infty < r_k < \eta_1 \\ \vdots & \\ L-1 & \eta_{(L-1)} < r_k < \infty \end{cases} \tag{3}$$

Let $\boldsymbol{\theta} = [x, y]^T$ be the source location to be estimated. Under the Gaussian noise assumption, the probability that D_k takes a specific value l is

$$p(D_k = l \,|\, \boldsymbol{\theta}) = Q\left(\frac{\eta_l - a_k}{\sigma}\right) - Q\left(\frac{\eta_{(l+1)} - a_k}{\sigma}\right) \tag{4}$$

where $Q(\cdot)$ is the complementary distribution function of the standard Gaussian distribution, and

$$Q(x) \triangleq \int_x^\infty \frac{1}{\sqrt{2\pi}} e^{-\frac{t^2}{2}}\, dt. \tag{5}$$

Let $\mathbf{D} = [D_1, D_2, \ldots, D_N]^T$ represent the collected data from all N sensors. Given the source location $\boldsymbol{\theta}$, the quantized sensor measurements are conditionally independent. Therefore, the likelihood function at the fusion center has the form [2]

$$p(\mathbf{D} \,|\, \boldsymbol{\theta}) = \prod_{k=1}^{N} \prod_{l=0}^{L-1} p(D_k = l \,|\, \boldsymbol{\theta})^{\delta(D_k - l)} \tag{6}$$

where $\delta(l)$ is the Kronecker delta function and is defined as

$$\delta(t) = \begin{cases} 1 & t = 0 \\ 0 & t \neq 0 \end{cases} \tag{7}$$

In this paper, we treat $\boldsymbol{\theta}$ as a random parameter which has a certain prior pdf. Therefore, we shall consider PCRLB as the estimation benchmark. Let $p(\mathbf{D}, \boldsymbol{\theta})$ be the joint probability density of the pair of $(\mathbf{D}, \boldsymbol{\theta})$. Then, the PCRLB of the estimation error has the form [26], [13]

$$E\{[\hat{\boldsymbol{\theta}}(\mathbf{D}) - \boldsymbol{\theta})][\hat{\boldsymbol{\theta}}(\mathbf{D}) - \boldsymbol{\theta})]^T\} \geq \mathbf{J}^{-1} \tag{8}$$

where $\mathbf{J}$ is the 2×2 Fisher information matrix (FIM)

$$\mathbf{J} = E\left[-\Delta_{\boldsymbol{\theta}}^{\boldsymbol{\theta}} \log p(\mathbf{D}, \boldsymbol{\theta})\right]. \tag{9}$$

In (9), $\Delta_{\boldsymbol{\theta}}^{\boldsymbol{\theta}} \triangleq \nabla_{\boldsymbol{\theta}} \nabla_{\boldsymbol{\theta}}^T$ is the second derivative operator, where $\nabla_{\boldsymbol{\theta}}$ is the gradient operator with respect to $\boldsymbol{\theta}$.

Using the equality $p(\mathbf{D}, \boldsymbol{\theta}) = p(\mathbf{D} \,|\, \boldsymbol{\theta}) p_0(\boldsymbol{\theta})$, an alternative expression for the Fisher information matrix can be written as

$$\mathbf{J} = E\left[-\Delta_{\boldsymbol{\theta}}^{\boldsymbol{\theta}} \log p(\mathbf{D} \,|\, \boldsymbol{\theta})\right] + E\left[-\Delta_{\boldsymbol{\theta}}^{\boldsymbol{\theta}} \log p_0(\boldsymbol{\theta})\right] = \mathbf{J}_d + \mathbf{J}_p \tag{10}$$

In (10), $\mathbf{J}_p \triangleq E[-\Delta_{\boldsymbol{\theta}}^{\boldsymbol{\theta}} \log p_0(\boldsymbol{\theta})]$ represents the *a priori* information, and $\mathbf{J_d} \triangleq E[-\Delta_{\boldsymbol{\theta}}^{\boldsymbol{\theta}} \log p(\mathbf{D} \,|\, \boldsymbol{\theta})]$ is the standard FIM averaged over the prior pdf of the source location as

$$\mathbf{J}_d = E\left[-\Delta_{\boldsymbol{\theta}}^{\boldsymbol{\theta}} \log p(\mathbf{D} \,|\, \boldsymbol{\theta})\right] = \int_\theta \mathbf{J}_s(\boldsymbol{\theta}) p_0(\boldsymbol{\theta}) d\theta. \tag{11}$$

Note that given the source location $\boldsymbol{\theta}$, $\mathbf{J}_s(\boldsymbol{\theta})$ is the standard FIM and according to [2] can be found as follows:

$$\mathbf{J}_s(\boldsymbol{\theta}) = n^2 \sum_{k=1}^{N} \kappa_k a_k^2 d_k^{-4} \times \begin{bmatrix} (x_k - x)^2 & (x_k - x)(y_k - y) \\ (x_k - x)(y_k - y) & (y_k - y)^2 \end{bmatrix} \tag{12}$$

where

$$\kappa_k = \frac{1}{8\pi\sigma^2} \sum_{l=0}^{L-1} \frac{\gamma_{i,l}}{p(D_k = l \,|\, \boldsymbol{\theta})}$$

and

$$\gamma_{k,l} = \left[e^{-\frac{(\eta_l - a_k)^2}{2\sigma^2}} - e^{-\frac{(\eta_{(l+1)} - a_k)^2}{2\sigma^2}}\right]^2.$$

In this paper, we assume that the prior probability density function (pdf) of the source location, $p_0(\boldsymbol{\theta})$, is $\mathcal{N}(\boldsymbol{\mu_0}, \boldsymbol{\Sigma}_0)$ where $\boldsymbol{\mu_0}$ is the center of the ROI and $\boldsymbol{\Sigma}_0 = \begin{bmatrix} \sigma_{x,0}^2 & 0 \\ 0 & \sigma_{y,0}^2 \end{bmatrix}$ is the covariance matrix which is very coarse so that its 99% confidence region covers the whole ROI. Note that our proposed approach

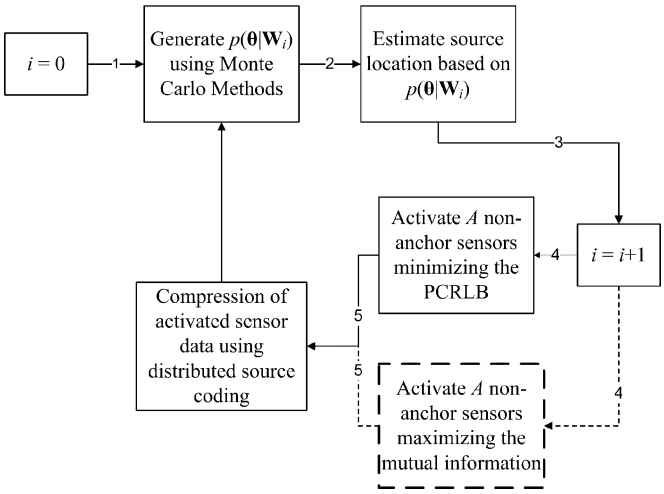

Fig. 2. The flow chart of the algorithm. The dashed blocks represents the state-of-the-art Mutual information based sensor selection method. The entire set of solid blocks represent the PCRLB based algorithm.

does not require the prior pdf to be Gaussian and will work with other prior pdfs also.

III. Iterative Source Location Estimation Method

Fig. 1 depicts an example WSN where each black point represents a sensor and the proposed iterative source localization algorithm is illustrated in Fig. 2. At step 1, the algorithm starts with the collection of M-bit quantized data from each of the K anchor sensors (represented with blue squares in Fig. 1). For notational simplicity, let $\mathbf{W}_i = [D_1, D_2, \ldots, D_{K+iA}]^T$ denote the collected sensor data until and including the ith iteration where $i \in \{0, 1, \ldots\}$ and A is the number of non-anchor sensors activated at each iteration (activated sensors are represented with green circles in Fig. 1 for the example considered in Section V). Note that, at iteration 0, only the anchor sensor data are received at the fusion center. Let $p(\boldsymbol{\theta} \,|\, \mathbf{W}_i)$ denote the posterior pdf of the source location based on the currently available sensor data $\mathbf{W}_i$ at the ith iteration. At step 2 of the algorithm shown in Fig. 2, the fusion center finds the source location estimate $\hat{\boldsymbol{\theta}}$ using the posterior pdf $p(\boldsymbol{\theta} \,|\, \mathbf{W}_i)$. The algorithm starts the next iteration $(i = i+1)$ at step 3 of the algorithm. Note that the posterior pdf of the source location is based on the previously received data until the end of iteration $i-1$ and $p(\boldsymbol{\theta} \,|\, \mathbf{W}_{i-1})$ serves as the prior pdf of source location for the ith iteration, which is denoted as $p_i(\boldsymbol{\theta})$

$$p_i(\boldsymbol{\theta}) = p(\boldsymbol{\theta} \,|\, \mathbf{W}_{i-1}). \tag{13}$$

At step 4 of the algorithm, the fusion center activates A non-anchor sensors. In this work, we present two sensor selection strategies. The first one selects the sensors that maximize the mutual information (MI) between the source location and sensors to be selected. The second one chooses the sensors that minimize the PCRLB. These two approaches will be compared in terms of computation complexity and mean squared error performance later in the paper. Finally, at step 5, using the already available sensor data as side information, the M-bit data of each activated sensor are locally compressed using standard distributed source coding techniques. We will show later through simulations that as the amount of information about the source location increases and the most informative (based on either the MI criterion or PCRLB criterion) sensors about the source location are selected, the estimation error on the source location decreases quickly.

A. Source Location Estimation Based on Monte Carlo Methods

At each iteration of the algorithm, the fusion center gathers the M-bit data (or its compressed version) from additional A non-anchor sensors. Let $p(\boldsymbol{\theta} \,|\, \mathbf{W}_i)$ be the posterior pdf of the source location given the available data $\mathbf{W}_i$ for iteration i, $i \geq 0$ (at step 1 in Fig. 2). In this paper, we approximate $p(\boldsymbol{\theta} \,|\, \mathbf{W}_i)$ using an importance sampling based Monte Carlo method [23], [27] as

$$p(\boldsymbol{\theta} \,|\, \mathbf{W}_i) = \sum_{m=1}^{N_s} w^{m,i} \delta(\boldsymbol{\theta} - \boldsymbol{\theta}^{m,i}) \tag{14}$$

where the posterior distribution of source location is represented by N_s particles and their weights. The particles $\boldsymbol{\theta}^{m,i} = [x^{m,i}\ y^{m,i}]^T$ $(m = 1, 2, \ldots, N_s)$ are drawn from the distribution $p_0(\boldsymbol{\theta})$ with equal weights $w^{m,0} = 1/N_s$. Let $\tilde{w}^{m,i}$ be the updated weight of particle $\boldsymbol{\theta}^{m,i}$ at the ith iteration which is obtained according to [23]

$$\tilde{w}^{m,i} \propto p(\mathbf{W}_i \,|\, \boldsymbol{\theta}^{m,i}) w^{m,0}. \tag{15}$$

The updated weight of each particle is then equal to the original weight multiplied by the likelihood function of the sensor data received up to the current iteration. Since the sensor decisions are conditionally independent, $p(\mathbf{W}_i \,|\, \boldsymbol{\theta}^{m,i}) = p(D_1 \,|\, \boldsymbol{\theta}^{m,i}) \times \ldots p(D_{K+iA} \,|\, \boldsymbol{\theta}^{m,i})$, and the likelihood function $p(\mathbf{W}_i \,|\, \boldsymbol{\theta}^{m,i})$ can be computed from (4) and (6). The particle weights are further normalized as

$$w^{m,i} = \frac{\tilde{w}^{m,i}}{\sum_{m=1}^{N_s} \tilde{w}^{m,i}}. \tag{16}$$

Then at the end of the ith iteration, the Monte Carlo approach yields the source location estimate $\hat{\boldsymbol{\theta}}_i$ as,

$$\hat{\boldsymbol{\theta}}_i = \sum_{m=1}^{N_s} w^{m,i} \boldsymbol{\theta}^{m,i}. \tag{17}$$

For the next iteration, the particles are generated from the prior $p_0(\boldsymbol{\theta})$ and weights are updated according to (15), using $\mathbf{W}_{i+1}$. Namely, we employ an importance-sampling based Monte Carlo method independently at each iteration using the entire received data to approximate the posterior distribution and update the source location. Having represented the posterior pdf of the source location, we can now describe the sensor selection methods.

B. Sensor Selection Methods

Let $\mathbf{S}_\mathbf{A}^i = \{\mathbf{s}_\mathbf{A}^{(1,i)}, \mathbf{s}_\mathbf{A}^{(2,i)}, \ldots, \mathbf{s}_\mathbf{A}^{(C_A^{N-K-(i-1)A}, i)}\}$ be the collection of all distinct A-element subsets of $N - K - (i-1)A$

remaining non-anchor sensors at iteration i. $C_A^{N-K-(i-1)A}$ is the combination operation. Let $\mathbf{s}_{\mathbf{A}}^{(\nu,i)}$ be the set of A non-anchor sensors activated at the ith iteration according to the sensor selection strategy ν. Then, $\mathbf{s}_{\mathbf{A}}^{(\nu,i)} = \{s_1^{\nu,i}, s_2^{\nu,i}, \ldots, s_A^{\nu,i}\}$ where $s_k^{\nu,i}$ $(k \in \{1, \ldots, A\})$ is the kth activated non-anchor sensor according to ν at iteration i and $\mathbf{D}_{\mathbf{A}}^{(\nu,i)} = \{D_1^{\nu,i}, D_2^{\nu,i}, \ldots, D_A^{\nu,i}\}$ are the quantized measurements of $\mathbf{s}_{\mathbf{A}}^{(\nu,i)}$. Now, the objective is to find the optimal sensor selection strategy ν^* which activates the set $\mathbf{s}_{\mathbf{A}}^{(\nu^*,i)} = \{s_1^{\nu^*,i}, s_2^{\nu^*,i}, \ldots, s_A^{\nu^*,i}\}$. Corresponding to the ith iteration, $\mathbf{s}_{\mathbf{A}}^{(\nu^*,i)}$ minimizes a certain cost function $\Psi_i(\cdot)$ as

$$\nu^* = \arg\min_{\mathbf{s}_{\mathbf{A}}^{(\nu,i)}} \Psi_i(\nu), \quad \nu \in \left\{1, 2, \ldots, C_A^{N-K-(i-1)A}\right\}. \tag{18}$$

In this work, we first select $\Psi_i(\nu)$ as the negative of the mutual information between source location and the sensors to be selected and then we select $\Psi_i(\nu)$ as the trace of the PCRLB matrix.

1) Mutual Information Based Sensor Selection: An entropy based sensor selection method using particle filters was presented in [12] where sensor data are assumed to be analog. In this section, we extend the approach presented in [12] to deal with quantized sensor data. Let $p_i(\boldsymbol{\theta})$ be the prior pdf of the source location as defined in (13). Besides the prior pdf of the source location, we also need to know the locations of non-anchor sensors and the sensing models of candidate sensors $p(\mathbf{D}_{\mathbf{A}}^{(\nu,i)} \,|\, \boldsymbol{\theta})$. Now, for iteration i, the objective is to find the optimal sensor activation scheme ν^* which activates A sensors out of $N - K - (i-1)A$ remaining non-anchor sensors whose data minimize the conditional entropy of the posterior source location distribution

$$\nu^* = \arg\min_{\nu} H\left(\boldsymbol{\theta} \,|\, \mathbf{D}_{\mathbf{A}}^{(\nu,i)}\right). \tag{19}$$

Let $I(\boldsymbol{\theta}, \mathbf{D}_{\mathbf{A}}^{(\nu,i)}) = H(\boldsymbol{\theta}) - H(\boldsymbol{\theta} \,|\, \mathbf{D}_{\mathbf{A}}^{(\nu,i)})$ be the mutual information between the source location $\boldsymbol{\theta}$ and the measurements of the activated sensors according to the activation scheme ν. The sensor selection problem now turns into

$$\nu^* = \arg\max_{\nu} I\left(\boldsymbol{\theta}, \mathbf{D}_{\mathbf{A}}^{(\nu,i)}\right). \tag{20}$$

$I(\boldsymbol{\theta}, \mathbf{D}_{\mathbf{A}}^{(\nu,i)})$ can also be expanded as,

$$I\left(\boldsymbol{\theta}, \mathbf{D}_{\mathbf{A}}^{(\nu,i)}\right) = H\left(\mathbf{D}_{\mathbf{A}}^{(\nu,i)}\right) - H\left(\mathbf{D}_{\mathbf{A}}^{(\nu,i)} \middle| \boldsymbol{\theta}\right). \tag{21}$$

To compute (21) using Monte Carlo approximation, we start with writing the entropy of $\mathbf{D}_{\mathbf{A}}^{(\nu,i)}$

$$H\left(\mathbf{D}_{\mathbf{A}}^{(\nu,i)}\right) = -\sum p\left(\mathbf{D}_{\mathbf{A}}^{(\nu,i)}\right) \log p\left(\mathbf{D}_{\mathbf{A}}^{(\nu,i)}\right). \tag{22}$$

$p(\mathbf{D}_{\mathbf{A}}^{(\nu,i)})$ can be decomposed as

$$p\left(\mathbf{D}_{\mathbf{A}}^{(\nu,i)}\right) = \int_{\theta} \left(\prod_{k=1}^{A} p\left(D_k^{\nu,i} \middle| \boldsymbol{\theta}\right)\right) p_i(\boldsymbol{\theta}) d\boldsymbol{\theta} \tag{23}$$

where $p_i(\boldsymbol{\theta})$ is the prior pdf of the source location and $p(D_1^{\nu,i} \,|\, \boldsymbol{\theta}), p(D_2^{\nu,i} \,|\, \boldsymbol{\theta}), \ldots, p(D_A^{\nu,i} \,|\, \boldsymbol{\theta})$ are the likelihood functions. Using (13) and (14) in (23) results in

$$\begin{aligned} p\left(\mathbf{D}_{\mathbf{A}}^{(\nu,i)}\right) &= \int_{\theta} \left(\prod_{k=1}^{A} p\left(D_k^{\nu,i} \middle| \boldsymbol{\theta}\right)\right) \\ &\quad \times \left(\sum_{m=1}^{N_s} w^{m,i-1} \delta\left(\boldsymbol{\theta} - \boldsymbol{\theta}^{m,i-1}\right)\right) d\boldsymbol{\theta} \\ &= \sum_{m=1}^{N_s} w^{m,i-1} \left(\prod_{k=1}^{A} p\left(D_k^{\nu,i} \middle| \boldsymbol{\theta}^{m,i-1}\right)\right). \end{aligned} \tag{24}$$

Then using (24), $H(\mathbf{D}_{\mathbf{A}}^{(\nu,i)})$ defined in (22) is rewritten as follows:

$$\begin{aligned} &H\left(\mathbf{D}_{\mathbf{A}}^{(\nu,i)}\right) \\ &= -\sum_{l_1=0}^{L-1} \cdots \sum_{l_A=0}^{L-1} \left\{\sum_{m=1}^{N_s} w^{m,i-1} \right. \\ &\quad \left. \times \left(\prod_{k=1}^{A} p\left(D_k^{\nu,i} = l_k \middle| \boldsymbol{\theta}^{m,i-1}\right)\right)\right\} \\ &\quad \times \log\left\{\sum_{m=1}^{N_s} w^{m,i-1} \left(\prod_{k=1}^{A} p\left(D_k^{\nu,i} = l_k \middle| \boldsymbol{\theta}^{m,i-1}\right)\right)\right\}. \end{aligned} \tag{25}$$

Now let us compute the second term of (21). First we have,

$$\begin{aligned} &H\left(\mathbf{D}_{\mathbf{A}}^{(\nu,i)} \middle| \boldsymbol{\theta}\right) \\ &\quad = -\int_{\boldsymbol{\theta}} \sum_{l_1, l_2, \ldots l_A} p\left(\mathbf{D}_{\mathbf{A}}^{(\nu,i)}, \boldsymbol{\theta}\right) \log p\left(\mathbf{D}_{\mathbf{A}}^{(\nu,i)} \middle| \boldsymbol{\theta}\right) d\boldsymbol{\theta} \end{aligned} \tag{26}$$

where $l_1, l_2, \ldots, l_A$ have been defined in (25). Since $p(\mathbf{D}_{\mathbf{A}}^{(\nu,i)}, \boldsymbol{\theta}) = p(\mathbf{D}_{\mathbf{A}}^{(\nu,i)} \,|\, \boldsymbol{\theta}) p_i(\boldsymbol{\theta})$, we have

$$\begin{aligned} &H\left(\mathbf{D}_{\mathbf{A}}^{(\nu,i)} \middle| \boldsymbol{\theta}\right) \\ &\quad = -\sum_{l_1=0}^{L-1} \cdots \sum_{l_A=0}^{L-1} \left(\int_{\theta} \left(\prod_{k=1}^{A} p\left(D_k^{\nu,i} = l_k \middle| \boldsymbol{\theta}\right)\right) p_i(\boldsymbol{\theta}) \right. \\ &\qquad \left. \times \log\left(\prod_{k=1}^{A} p\left(D_k^{\nu,i} = l_k \middle| \boldsymbol{\theta}\right)\right) d\boldsymbol{\theta}\right). \end{aligned} \tag{27}$$

Then using the Monte Carlo approximation of the prior source location pdf, $H(\mathbf{D}_{\mathbf{A}}^{(\nu,i)} \,|\, \boldsymbol{\theta})$ becomes

$$\begin{aligned} &H\left(\mathbf{D}_{\mathbf{A}}^{(\nu,i)} \middle| \boldsymbol{\theta}\right) \\ &\quad = -\sum_{k=1}^{A} \sum_{l=0}^{L-1} \left[\int_{\theta} p\left(D_k^{\nu,i} = l \middle| \boldsymbol{\theta}\right) \right. \\ &\qquad \times \left\{\sum_{m=1}^{N_s} w^{m,i-1} \delta(\boldsymbol{\theta} - \boldsymbol{\theta}^{m,i-1})\right\} \\ &\qquad \left. \times \log\left(p\left(D_k^{\nu,i} = l \middle| \boldsymbol{\theta}\right)\right) d\boldsymbol{\theta}\right] \\ &\quad = -\sum_{k=1}^{A} \sum_{l=0}^{L-1} \left[\sum_{m=1}^{N_s} w^{m,i-1} p\left(D_k^{\nu,i} = l \middle| \boldsymbol{\theta}^{m,i-1}\right) \right. \\ &\qquad \left. \times \log\left(p\left(D_k^{\nu,i} = l \middle| \boldsymbol{\theta}^{m,i-1}\right)\right)\right]. \end{aligned} \tag{28}$$

Finally using (25) and (28), the mutual information function $I(\boldsymbol{\theta}, \mathbf{D}_{\mathbf{A}}^{(\nu,i)})$ expressed in (21) is calculated as

$$I\left(\boldsymbol{\theta}, \mathbf{D}_{\mathbf{A}}^{(\nu,i)}\right) = -\sum_{l_1=0}^{L-1} \cdots \sum_{l_A=0}^{L-1} \left[\left\{ \sum_{m=1}^{N_s} w^{m,i-1} \left(\prod_{k=1}^{A} p\left(D_k^{\nu,i} = l_k \middle| \boldsymbol{\theta}^{m,i-1} \right) \right) \right\} \times \log \left\{ \sum_{m=1}^{N_s} w^{m,i-1} \left(\prod_{k=1}^{A} p\left(D_k^{\nu,i} = l_k \middle| \boldsymbol{\theta}^{m,i-1} \right) \right) \right\} \right] + \left[\sum_{k=1}^{A} \sum_{l=0}^{L-1} \left\{ \sum_{m=1}^{N_s} w^{m,i-1} p\left(D_k^{\nu,i} = l \middle| \boldsymbol{\theta}^{m,i-1} \right) \times \log \left(p\left(D_k^{\nu,i} = l \middle| \boldsymbol{\theta}^{m,i-1} \right) \right) \right\} \right]. \quad (29)\text{–}(30)$$

The quantity $-I(\boldsymbol{\theta}, \mathbf{D}_{\mathbf{A}}^{(\nu,i)})$ is employed as $\Psi_i(\nu)$ for sensor selection in (18).

2) PCRLB Based Sensor Selection: After initialization via the use of K anchor sensors, during each iteration the fusion center requests data from A non-anchor sensors that minimize the PCRLB. At iteration i, given available data $\mathbf{W}_{i-1}$, the PCRLB of A non-anchor sensors is expressed as

$$E\{(\hat{\boldsymbol{\theta}} - \boldsymbol{\theta})(\hat{\boldsymbol{\theta}} - \boldsymbol{\theta})^T \,|\, \mathbf{W}_{i-1}\} \geq F^{-1}\left(\mathbf{D}_{\mathbf{A}}^{(\nu,i)} \middle| \mathbf{W}_{i-1} \right) \quad (31)$$

where $\mathbf{J}_c(\nu) = F(\mathbf{D}_{\mathbf{A}}^{(\nu,i)} \,|\, \mathbf{W}_{i-1})$ is the FIM of the random variable $\boldsymbol{\theta}$ contained in $\mathbf{D}_{\mathbf{A}}^{(\nu,i)}$ given available data $\mathbf{W}_{i-1}$. Then $\mathbf{J}_c(\nu)$ is expressed as

$$\begin{aligned} \mathbf{J}_c(\nu) &= F\left(\mathbf{D}_{\mathbf{A}}^{(\nu,i)} \middle| \mathbf{W}_{i-1} \right) \\ &\triangleq E\left\{ \left[-\Delta_{\boldsymbol{\theta}}^{\boldsymbol{\theta}} \log p\left(\boldsymbol{\theta}, \mathbf{D}_{\mathbf{A}}^{(\nu,i)} \middle| \mathbf{W}_{i-1} \right) \right] \middle| \mathbf{W}_{i-1} \right\} \\ &= -\int_{\boldsymbol{\theta}} \sum_{l_1, l_2, \ldots, l_A} \left[\Delta_{\boldsymbol{\theta}}^{\boldsymbol{\theta}} \log p\left(\boldsymbol{\theta}, \mathbf{D}_{\mathbf{A}}^{(\nu,i)} \middle| \mathbf{W}_{i-1} \right) \right] \\ &\quad \times p\left(\boldsymbol{\theta}, \mathbf{D}_{\mathbf{A}}^{(\nu,i)} \middle| \mathbf{W}_{i-1} \right) d\boldsymbol{\theta} \end{aligned} \quad (32)$$

where we take expectation over all possible source locations $\boldsymbol{\theta}$ and all quantized sensor measurements $\{l_1, l_2, \ldots, l_A\}$.

Using Bayesian decomposition, the joint probability density function $p(\boldsymbol{\theta}, \mathbf{D}_{\mathbf{A}}^{(\nu,i)} \,|\, \mathbf{W}_{i-1})$ of source location $\boldsymbol{\theta}$ and new quantized measurements $\mathbf{D}_{\mathbf{A}}^{(\nu,i)}$ is written as

$$p\left(\boldsymbol{\theta}, \mathbf{D}_{\mathbf{A}}^{(\nu,i)} \middle| \mathbf{W}_{i-1} \right) = p\left(\mathbf{D}_{\mathbf{A}}^{(\nu,i)} \middle| \boldsymbol{\theta} \right) p(\boldsymbol{\theta} \,|\, \mathbf{W}_{i-1}) \quad (33)$$

where the identity $p(\mathbf{D}_{\mathbf{A}}^{(\nu,i)} \,|\, \mathbf{W}_{i-1}, \boldsymbol{\theta}) = p(\mathbf{D}_{\mathbf{A}}^{(\nu,i)} \,|\, \boldsymbol{\theta})$ has been used. Using the properties $p(\mathbf{D}_{\mathbf{A}}^{(\nu,i)} \,|\, \boldsymbol{\theta}) = \prod_{k=1}^{A} p(D_k^{\nu,i} \,|\, \boldsymbol{\theta})$ and $\sum_{l_1, l_2, \ldots, l_A} p(\mathbf{D}_{\mathbf{A}}^{(\nu,i)} \,|\, \boldsymbol{\theta}) = 1$, (32) reduces to,

$$\begin{aligned} \mathbf{J}_c(\nu) = -\Bigg\{ &\int_{\boldsymbol{\theta}} \sum_{k=1}^{A} \sum_{l=0}^{L-1} \left\{ \left[\Delta_{\boldsymbol{\theta}}^{\boldsymbol{\theta}} \log p\left(D_k^{\nu,i} = l \middle| \boldsymbol{\theta} \right) \right] \right. \\ &\left. \times\, p\left(D_k^{\nu,i} = l \middle| \boldsymbol{\theta} \right) \right\} p(\boldsymbol{\theta} \,|\, \mathbf{W}_{i-1}) d\boldsymbol{\theta} \\ &+ \int_{\boldsymbol{\theta}} \left[\Delta_{\boldsymbol{\theta}}^{\boldsymbol{\theta}} \log p(\boldsymbol{\theta} \,|\, \mathbf{W}_{i-1}) \right] p(\boldsymbol{\theta} \,|\, \mathbf{W}_{i-1}) d\boldsymbol{\theta} \Bigg\}. \end{aligned} \quad (34)$$

Note that the result of the double summation, $-\sum_{k=1}^{A} \sum_{l=0}^{L-1} [\Delta_{\boldsymbol{\theta}}^{\boldsymbol{\theta}} \log p(D_k^{\nu,i} = l \,|\, \boldsymbol{\theta})] p(D_k^{\nu,i} = l \,|\, \boldsymbol{\theta})$, has been derived in [2] and provided by (12). For the first term of (34), we use (13) and (14) to approximate $p(\boldsymbol{\theta} \,|\, \mathbf{W}_{i-1})$. The second term requires the second derivative of $p(\boldsymbol{\theta} \,|\, \mathbf{W}_{i-1})$. Since $p(\boldsymbol{\theta} \,|\, \mathbf{W}_{i-1})$ has a non-parametric representation by a set of random samples with associated weights, it is very difficult to express the exact form of its second order derivatives. Instead we compute the second term in (34) numerically. Let us define,

$$\boldsymbol{\Gamma}_i \triangleq \int_{\boldsymbol{\theta}} \left[\Delta_{\boldsymbol{\theta}}^{\boldsymbol{\theta}} \log p(\boldsymbol{\theta} \,|\, \mathbf{W}_{i-1}) \right] p(\boldsymbol{\theta} \,|\, \mathbf{W}_{i-1}) d\boldsymbol{\theta}. \quad (35)$$

We can calculate the (1,1) element of $\boldsymbol{\Gamma}_i$ first.

$$\boldsymbol{\Gamma}_i(1,1) = -\int_x \int_y \frac{1}{p(\boldsymbol{\theta} \,|\, \mathbf{W}_{i-1})} \left(\frac{\partial p(\boldsymbol{\theta} \,|\, \mathbf{W}_{i-1})}{\partial x} \right)^2 dy dx$$

Let $\mathcal{A}^2$ be the area of the region of interest (ROI). We partition the ROI into G equal size cells where the area of each cell is $\xi^2 = \mathcal{A}^2/G$ and ξ is the distance between the centers of each neighboring cell.

Let $p(\boldsymbol{\theta} \in \{c, q\} \,|\, \mathbf{W}_{i-1})$ be the probability of a particular cell specified by the cell indexes c and q, then

$$\begin{aligned} &p(\boldsymbol{\theta} \in \{c, q\} \,|\, \mathbf{W}_{i-1}) \\ &\quad = p\left\{ x^{m,i} \in [c\xi, (c+1)\xi] \;\&\; y^{m,i} \in [q\xi, (q+1)\xi] \right\} \end{aligned}$$

where

$$c \in \{0, 1, \ldots, \sqrt{G} - 1\},\ q \in \{0, 1, \ldots, \sqrt{G} - 1\}.$$

Denote $V_{c,q}$ as the total number of particles inside the cell specified by c and q where each particle has the weight $w_v^{c,q}$. Then,

$$p(\boldsymbol{\theta} \in \{c, q\} \,|\, \mathbf{W}_{i-1}) = \sum_{v=1}^{V_{c,q}} w_v^{c,q}. \quad (36)$$

Then $\boldsymbol{\Gamma}_i(1,1)$ can be approximated as follows:

$$\boldsymbol{\Gamma}_i(1,1) \approx -\sum_{c=0}^{\sqrt{G}-1} \sum_{q=0}^{\sqrt{G}-1} \frac{1}{p(\boldsymbol{\theta} \in \{c, q\} \,|\, \mathbf{W}_{i-1})} \left(\frac{p(\boldsymbol{\theta} \in \{c+1, q\} \,|\, \mathbf{W}_{i-1}) - p(\boldsymbol{\theta} \in \{c, q\} \,|\, \mathbf{W}_{i-1})}{\xi} \right)^2 \xi^2. \quad (37)$$

Using the above procedure $\boldsymbol{\Gamma}_i(1,2)$, $\boldsymbol{\Gamma}_i(2,1)$ and $\boldsymbol{\Gamma}_i(2,2)$ can be computed similarly. Note that the calculation of $\boldsymbol{\Gamma}_i$ is independent of the number of sensors to be selected (A).

Using the approximations presented in (14) and (37), (34) is rewritten as follows:

$$\begin{aligned} &\mathbf{J}_c(\nu) \\ &\quad = -\left[\left\{ \sum_{m=1}^{N_s} w^{m,i-1} \sum_{k=1}^{A} \sum_{l=0}^{L-1} \left[\Delta_{\boldsymbol{\theta}}^{\boldsymbol{\theta}} \log p\left(D_k^{\nu,i} = l \middle| \boldsymbol{\theta}^{m,i-1} \right) \right] \right. \right. \\ &\qquad \left. \left. \times\, p\left(D_k^{\nu,i} = l \middle| \boldsymbol{\theta}^{m,i-1} \right) \right\} + \boldsymbol{\Gamma}_i \right]. \end{aligned} \quad (38)$$

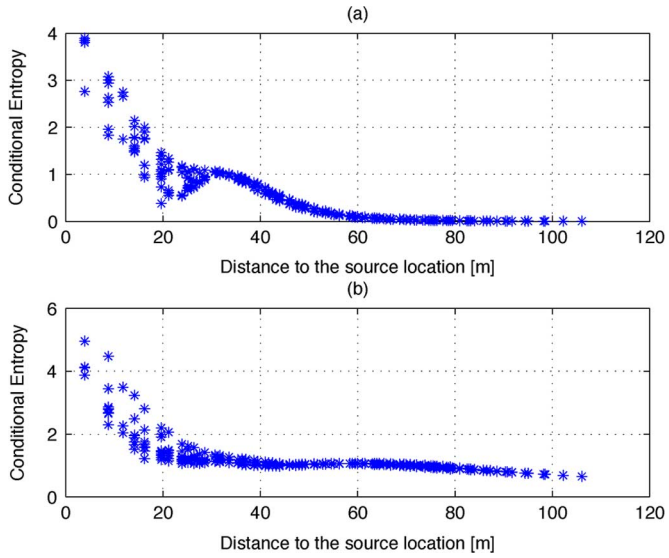

Fig. 3. Conditional Entropy of non-anchor sensors in the field given the multi-bit decisions of the anchor sensors at the beginning of the first iteration. (a) $M = 5$ bit, (b) $M = 6$ bit.

The result of the two inner summations in the first term of (38) is basically the negative of the FIM defined in (12) which is then averaged over the prior distribution of the source location represented by the particles. For the activation strategy ν, we calculate its corresponding FIM $\mathbf{J}_c(\nu)$ as defined in (38). The fusion center then decides on the optimal sensor activation strategy ν^* that minimizes the trace of $\mathbf{J}_c^{-1}(\nu)$ which is the PCRLB corresponding to the summation of the MSEs of the estimates of x and y.

Note that the mutual information function defined in (29) requires $N_s \times L^A + A \times L \times N_s$ summations. In comparison, the FIM function defined in (38) requires $A \times L \times N_s$ summations. In other words, since (29) requires an A-fold summation, the complexity of the mutual information increases exponentially with A while the computational complexity of PCRLB increases linearly with A.

IV. Sensor Data Compression

In this section, distributed source coding techniques are discussed which use the prior pdf of the source location to further compress the data transmitted by the activated sensors. Let $s_k^{\nu^*,i}$, $(k \in \{1, 2, \ldots, A\})$ be a non-anchor sensor which is activated according to the sensor selection strategy ν^* at iteration i. Using the Monte Carlo approximation of the prior pdf of the source location, probability of receiving a certain data l from $s_k^{\nu^*,i}$ is $p(D_k^{\nu^*,i} = l)$ and expressed as

$$p\left(D_k^{\nu^*,i} = l\right) = \int_{\boldsymbol{\theta}} p\left(D_k^{\nu^*,i} = l \middle| \boldsymbol{\theta}\right) p_i(\boldsymbol{\theta}) d\boldsymbol{\theta} = \sum_{m=1}^{N_s} w^{m,i-1} p\left(D_k^{\nu^*,i} = l \middle| \boldsymbol{\theta}^{m,i-1}\right). \quad (39)$$

Let $H(D_k^{\nu^*,i})$ [28] be the conditional entropy of a non-anchor sensor $D_k^{\nu^*,i}$ which is defined as,

$$H\left(D_k^{\nu^*,i}\right) = -\sum_{l=0}^{L-1} p\left(D_k^{\nu^*,i} = l\right) \log_2 p\left(D_k^{\nu^*,i} = l\right). \quad (40)$$

The fusion center requests the M-bit data of each non-anchor sensor to be activated in B_k bits, where B_k has to satisfy

$$B_k \geqslant H\left(D_k^{\nu^*,i}\right) \quad k \in \{1, 2, \ldots, A\}. \quad (41)$$

As an example, in Fig. 3, we present the conditional entropies of $N - K = 345$ non-anchor sensors for the first iteration given the decisions of $K = 16$ anchor sensors as depicted in Fig. 1 and the source is located at [75 m. 75 m.]. Simulation results show that the sensors close to the actual source location have high entropies. When $M = 5$, as the sensor distance from the source location increases, quantized observations of the sensors tend to zero and no matter what the side information is, conditional entropy of such a sensor decreases and goes to zero. Note that for the $M = 6$ bit case, the asymptotic entropy of each non-anchor sensor far away from the source is around 1 due to the noise fluctuations. This means that only a small subset of the sensors contain information of the source location.

In this paper, we select

$$B_k = \min\left\{\left(\left\lceil H\left(D_k^{\nu^*,i}\right)\right\rceil + 1\right), M\right\} \quad (42)$$

where $\lceil \cdot \rceil$ is the round towards next integer operator or the ceiling function. Using an approximate prior pdf for the source location makes the conditional entropy of each sensor defined in (40) also approximate. According to the structure of our iterative method, any decoding error at a particular iteration may cause error propagation at the subsequent iterations. Therefore, in order to ensure lossless data compression, we include an extra guard bit to the approximated entropy of each sensor to be activated.

Let u_k be the B_k-bit compressed sensor data which is obtained from its actual M-bit sensor observation $D_k^{\nu^*,i}$ according to [24] as

$$u_k = D_k^{\nu^*,i} \bmod 2^{B_k} \quad (43)$$

where we assume that u_k is delivered to the fusion center without any error.

The fusion center generates the decision vector L_u which includes all the possible multi-bit decisions ls that yield u_k as a remainder after the modulo 2^{B_k} operation:

$$L_u = [l : \forall l, \quad u_k = l \bmod 2^{B_k}]. \quad (44)$$

Using the past information $\mathbf{W}_{i-1}$ as side information, the multi-bit decision of each sensor is recovered with a simple maximum *a posteriori* probability (MAP) rule

$$l^* = \arg\max_{l \in L_u} p\left(D_k^{\nu^*,i} = l \middle| \mathbf{W}_{i-1}\right) \quad (45)$$

TABLE I
MEAN CPU TIMES OF MI AND PCRLB

	PCRLB	MI
$A = 1$	0.26 s.	0.17 s.
$A = 2$	0.51 s.	9.49 s.
$A = 3$	0.75 s.	371.79 s.
$A = 4$	1.00 s.	15544.00 s.

where $p(D_k^{\nu^*,i} = l \,|\, \mathbf{W}_{i-1})$ is calculated according to (39). As an example, suppose that $M = 4$ and $L = 2^4$. Let the quantized data of an activated sensor be $D_k = 12$. If the quantized data of the activated sensor is requested in $B_k = 3$ bits, then $u_k = 12 \bmod 2^3$. Fusion center receives $u_k = 4$, finds out that $L_u = \{4, 12\}$ and computes the following probabilities, $p(D_k = 4 \,|\, \mathbf{W}_{i-1})$ and $p(D_k = 12 \,|\, \mathbf{W}_{i-1})$ according to (39). The fusion center then picks either 4 or 12, depending on which has the largest probability.

After recovering the decision of each activated sensor, $D_k^{\nu^*,i} = l^*$, at iteration i, the fusion center updates the new posterior pdf $p(\boldsymbol{\theta} \,|\, \mathbf{W}_i)$ using the procedure described in Section III-A.

V. SIMULATION RESULTS

In this section, we first compare the computational cost of the two sensor selection schemes presented, then we give some illustrative examples to show their source location estimation performances. Tradeoff between estimation performance and communication cost is also studied.

A. Computational Cost

In this subsection, we compare the computation times of the two sensor selection metrics. The mutual information based sensor selection method uses (29) to calculate the mutual information between the source location and the sensor measurements. The PCRLB based sensor selection method uses (38) and calculates the trace of the PCRLB matrix. We use MATLAB's `cputime` function to evaluate the computation times of functions (29) and (38). Table I shows the average computation times of the two methods. The results are averaged over 100 different executions of each function. The CPU times are obtained on a computer with 2.1 GHz processor.

For $A = 1$, (29) is much simpler than (38), so (29) is computed faster than (38). On the other hand, for $A \geq 2$, the computational complexity of MI increases exponentially with A as L^A while the computation time of PCRLB increases linearly with A as $L \times A$. Note that for the ith iteration of the algorithm, the selection of A optimal sensors has a search set of size $C_A^{N-K-(i-1)A}$ which is the same for the two sensor selection schemes. In a dense network, activating a large number of sensors may result in a large search space and it may take a long time to find the optimal sensor selection strategy.

B. Algorithm Performance

In our examples, we consider the source energy and signal decay exponent as $P_0 = 25\,000$ and $n = 2$ respectively. $N = 19 \times 19 = 361$ sensors are deployed in a 100×100 m^2 field and the sensors are deployed in a grid where the location of each sensor is assumed to be known. The selection of K is determined by the event detection performance which is not studied in this paper. A small value of K may result in a situation where none of the anchor sensors receive the signal from the source. On the other hand, a relatively large value for K may yield an accurate source location estimate so further improvement of the location estimate may no longer be necessary. In this paper, the iterative algorithm is initialized with $K = 4 \times 4 = 16$ anchor sensors deployed in a grid layout, covering the ROI. We assume that each sensor in the field uses the same decision thresholds. The optimal quantization rules for M-bit sensor data are given in [2]. On the other hand, such rules mostly affect the performance when the number of decision intervals $L = 2^M$ is small (e.g., for the cases when $M = 1$ or $M = 2$). Since we are interested in a large number of quantization levels $(M \geq 3)$, the optimal design of decision thresholds becomes less crucial. Therefore, we select $L-1$ points as the quantization thresholds which evenly partition the interval $[0, \sqrt{P_0}]$. The sensor measurements less than 0 and more than $\sqrt{P_0}$ are mapped to 0 and $L-1$ respectively. In order to compute (37), we select $\sqrt{G} = 100$ and $\xi = 1$ m.

Before the first iteration, the prior pdf of the source location $p_0(\boldsymbol{\theta})$ is assumed to be a Gaussian with $\mathcal{N}(\boldsymbol{\mu}_0, \boldsymbol{\Sigma}_0)$ where $\boldsymbol{\mu}_0 = [50 \text{ m}. \; 50 \text{ m}.]^T$ and $\boldsymbol{\Sigma}_0 = \begin{bmatrix} \sigma_{x,0}^2 & 0 \\ 0 & \sigma_{y,0}^2 \end{bmatrix}$ where $3\sigma_{x,0} = 3\sigma_{y,0} = 50$ m. and $\mathbf{J}_{p_0} = \boldsymbol{\Sigma}_0^{-1}$. We select $N_s = 10\,000$ particles and the particles $\boldsymbol{\theta}^{m,i}$ are also drawn from $\mathcal{N}(\boldsymbol{\mu}_0, \boldsymbol{\Sigma}_0)$ where $w^{m,0} = 1/N_s$. The mean square error (MSE) matrix of the estimation is calculated as follows:

$$\text{MSE} = \frac{1}{Z} \sum_{z=1}^{Z} (\hat{\boldsymbol{\theta}}_z - \boldsymbol{\theta}_z)(\hat{\boldsymbol{\theta}}_z - \boldsymbol{\theta}_z)^T. \tag{46}$$

We tested our algorithm over $Z = 100$ different source locations $\boldsymbol{\theta}_{\boldsymbol{z}}$ drawn from the prior distribution $\mathcal{N}(\boldsymbol{\mu}_0, \boldsymbol{\Sigma}_0)$.

1) Estimation Performance: In Fig. 4, we present the MSE of estimation using MI and PCRLB based sensor selection methods without employing data compression at each activated sensor. The experimental MSE obtained above is also compared with the PCRLB found when all the $N = 361$ sensors send their M-bit quantized data to the fusion center as defined in (10). In our simulations, we activate $A = 1$ sensor at a time after the initialization via anchor sensors.

For performance comparison, we also consider selecting A sensors which are the nearest to the source location estimate $\hat{\boldsymbol{\theta}}$ obtained from the previous iteration. Simulation results show that, when $M = 3$, the MI and PCRLB based sensor selection schemes are the best sensor selection schemes and outperform the nearest sensor selection scheme in terms of MSE. For $M = 5$, measurements of each activated sensor become more informative and the nearest, MI and PCRLB based sensor selection schemes achieve similar performance. Instead of using $N = 361$ sensors, in 5 iterations 21 sensors are enough to achieve a performance close to that when all the $N = 361$ sensors send their data to the fusion center. In Fig. 5, we present the trace of the MSE matrix of estimation using MI and PCRLB based sensor selection methods. The experimental MSE is also

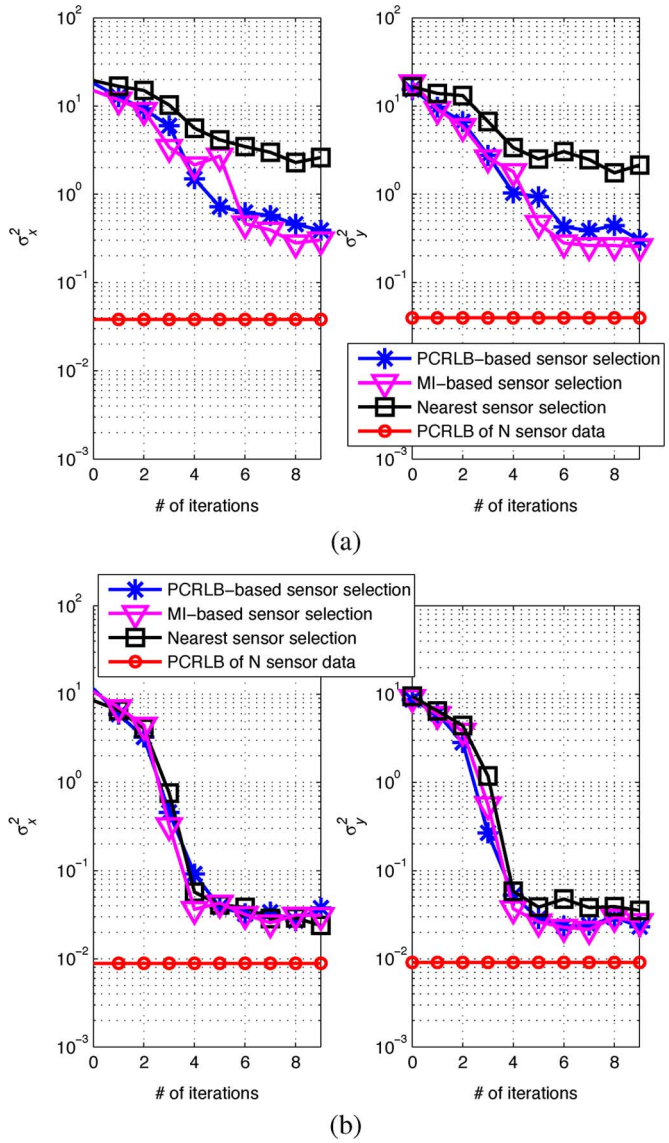

Fig. 4. MSE at each iteration. Sensor selection is based on MI, PCRLB and nearest sensor to the estimated source location. (a) $M = 3$, (b) $M = 5$ bits quantization. $A = 1$.

compared with the trace of the PCRLB matrix found when all $N = 361$ sensors send their $M = 5$-bit quantized data to the fusion center. In both cases of $A = 1$ and $A = 2$, the PCRLB-based sensor selection method yields similar MSE performance as that of MI-based sensor selection method.

2) Data Compression Performance: In Table II, we compare the MSE of the location estimate at the end of the 9th iteration obtained based on compressed data to that based on data without compression. Source localization with compressed data achieves almost the same performance as that without data compression, which implies that the compressed sensor measurements are decoded almost perfectly at each iteration. For performance evaluation, we define two metrics: For iteration i, compression gain $(\mathrm{CG}_M(i))$ is the ratio between average reduction in the number of transmitted bits and the fixed number of bits$M$

$$\mathrm{CG}_M(i) = 1 - \frac{\bar{B}_k(i)}{M} \tag{47}$$

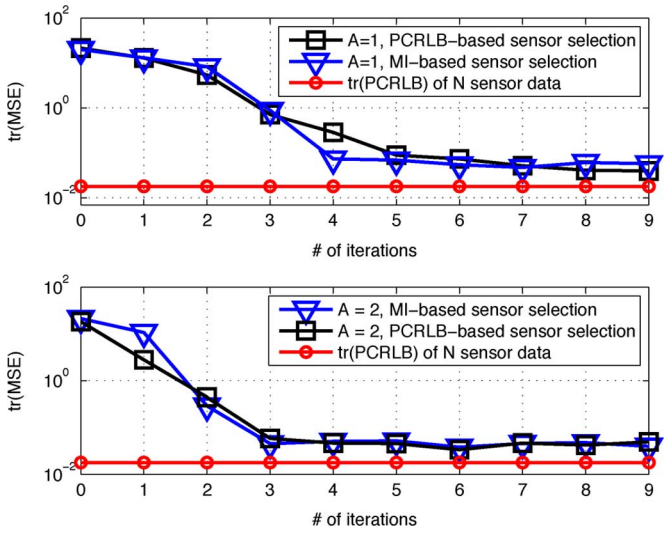

Fig. 5. MSE performance of MI and PCRLB based sensor selection schemes. $N = 361$, $K = 16$, $M = 5$, $A = 1$ and $A = 2$ sensor activations/iteration.

TABLE II
MSE AT THE END OF THE 9TH ITERATION. ($A = 1$, PCRLB BASED SENSOR SELECTION IS APPLIED)

	$M = 3$ x axis	$M = 3$ y axis	$M = 5$ x axis	$M = 5$ y axis
No Data Compression	0.3888	0.2993	0.0270	0.0296
Data Compression	0.3369	0.1775	0.0314	0.0259
PCRLB of N sensor data	0.0381	0.0396	0.0089	0.0091

where $\bar{B}_k(i)$ is the average number of bits transmitted to the fusion center at the ith iteration.

The overall compression gain (OCG_M) is then defined as the average reduction in the total number of transmitted bits and the fixed number of M bits until the end of the ninth iteration:

$$\mathrm{OCG}_M = 1 - \frac{\sum_{i=1}^{9} \bar{B}_k(i)}{9M}. \tag{48}$$

Results presented in Table III show that, for $M \geq 5$, over 9 iterations, about 40% of the bits are saved by compression. At the beginning of the algorithm there is a relatively large uncertainty about the source location, so the measurements of the sensors selected at the beginning of the algorithm are transmitted to the fusion center in almost M-bits. This is why CG is small during the first few iterations. For the particular case illustrated in Fig. 4, after the 3rd iteration, the MSE of the location estimate decreases rapidly which is the time when most of the informative sensors about the source location are selected. Then there is no need to send full M-bit information to the fusion center. As the fusion center learns more about the source location and the most informative sensors have been selected, the uncertainty regarding source location gets smaller, and the conditional entropy defined in (40) becomes very small. After the most informative sensors have been selected, the CG increases to around 50% for $M = 5$ and $M = 6$.

C. The Tradeoff Between Estimation Performance and Communication Cost

In order to make the proposed iterative algorithm useful in practice, we introduce a stopping criterion to terminate the it-

TABLE III
AVERAGE NUMBER OF BITS USED TO REPRESENT THE SENSOR DATA ($A = 1$)

Iteration	$M = 3$	CG_3	$M = 5$	CG_5	$M = 6$	CG_6
1	3.00	0	4.50	0.10	5.87	0.02
2	2.99	0	4.90	0.02	5.85	0.03
3	2.86	0.05	4.16	0.16	4.27	0.29
4	2.53	0.16	2.97	0.40	3.22	0.46
5	2.22	0.26	2.29	0.54	2.97	0.51
6	2.10	0.30	2.09	0.58	2.92	0.51
7	2.05	0.32	2.02	0.59	2.94	0.51
8	2.00	0.33	2.01	0.60	2.90	0.52
9	2.00	0.33	2.00	0.60	2.84	0.53
OCG	-	0.19	-	0.40	-	0.37

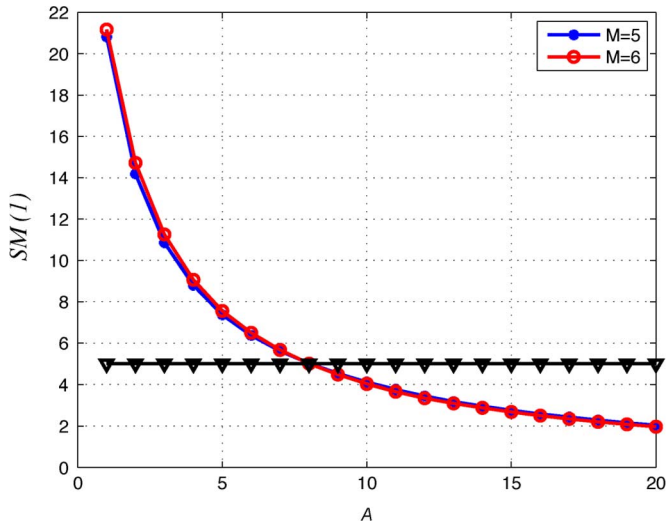

Fig. 6. Stopping metric versus the number of sensors to be selected. The black line with triangle markers indicates the accuracy threshold ($i = 1, \epsilon = 5$).

erations. Since the sensor placements are known and the prior distribution of source location is available, the fusion center can compute the PCRLB of the source location estimate. Let $\mathrm{tr}\{\mathrm{MSE}(N)\}$ be the trace of the MSE matrix when data from all the N sensors are assumed to be received and let $\mathrm{tr}\{\mathrm{MSE}(K + iA)\}$ be the MSE after data from $K + iA$ sensors are received. Then $\mathcal{SM}(i)$ is defined as the stopping metric at iteration i, and the iterative algorithm terminates after the following criterion is met:

$$\mathcal{SM}(i) = \frac{\mathrm{tr}\{\mathrm{MSE}(K + iA)\} - \mathrm{tr}\{\mathrm{MSE}(N)\}}{\mathrm{tr}\{\mathrm{MSE}(N)\}} \leq \epsilon \quad (49)$$

where ϵ is the desired accuracy.

1) Offline Evaluation of Stopping Metric: The stopping metric (49) can be computed offline using the initial prior pdf $(\mathcal{N}(\boldsymbol{\mu}_0, \boldsymbol{\Sigma}_0))$. It can be used by the fusion center to coarsely determine how many and which non-anchor sensors should be selected to meet the stopping criterion in advance. Since PCRLB is a lower bound on the MSE and the MSE gets very close to its PCRLB for large sensor data, $\mathrm{tr}\{\mathrm{MSE}(N)\}$ can be approximated[1] by its PCRLB as $\mathrm{tr}\{\mathrm{MSE}(N)\} \approx \mathrm{tr}\{\mathrm{PCRLB}(N)\}$. At each iteration, similarly we assume that $\mathrm{tr}\{\mathrm{MSE}(K + iA)\} \approx \mathrm{tr}\{\mathrm{PCRLB}(K + iA)\}$. Given the prior distribution of the source location $(\mathcal{N}(\boldsymbol{\mu}_0, \boldsymbol{\Sigma}_0))$, appropriate selection of the number and locations of sensors in the network, and the number and locations of the anchor sensors yields significant communication savings as compared to one-shot location estimation. As shown in Fig. 6, $\mathcal{SM}(1)$ intersects the threshold at about 9. Therefore, 9 sensors should be selected to meet the stopping criterion at the first iteration.

2) Online Evaluation of Stopping Metric: We next evaluate the number of iterations and the communication cost by evaluating the stopping metric (49) online. We select A non-anchor sensors at each iteration based on the PCRLB-based sensor selection metric. $\mathcal{SM}(i)$ for the selected sensors at iteration i is computed online using the iteratively refined posterior pdf. To compute the MSE of all sensor data, we use the approximation $\mathrm{tr}\{\mathrm{MSE}(N)\} \approx \mathrm{tr}\{\mathrm{PCRLB}(N)\}$. $\mathrm{tr}\{\mathrm{MSE}(K + iA)\}$ is approximated using the iteratively refined posterior pdf as

$$\mathrm{tr}\{\mathrm{MSE}(K + iA)\} \approx \mathrm{tr}\{\boldsymbol{\Sigma}_i\}$$

where

$$\boldsymbol{\Sigma}_i = \sum_{m=1}^{N_s} w^{m,i}(\boldsymbol{\theta}^{m,i} - \boldsymbol{\mu}_i)(\boldsymbol{\theta}^{m,i} - \boldsymbol{\mu}_i)^T$$

and

$$\boldsymbol{\mu}_i = \sum_{m=1}^{N_s} w^{m,i}\boldsymbol{\theta}^{m,i}$$

Fig. 7(a) shows the average number of iterations which is required for the stopping criterion (49) to be satisfied versus A. For $A = 1$ and $M = 5$, the algorithm terminates in about five iterations which is consistent with Fig. 4(b). According to offline computation of $\mathcal{SM}(i)$, 9 sensors need to be selected in order for the MSE to get very close to the PCRLB of N sensor data. Therefore, the offline computation of $\mathcal{SM}(i)$ yields a loose estimate of the required number of iterations. The results presented in Fig. 7(b) show the average total number of bits used by the non-anchor sensors until the end of the iterations by activating the sensors based on iteratively updated posterior pdf of the source location and using distributed source coding. As A increases, the algorithm terminates much faster, at the cost of increased total number of bits transmitted to the fusion center. As an example, for $M = 5$ and $A = 1$, the algorithm terminates in about 5 iterations and on the average 20 bits are transmitted to the fusion center. For $M = 5$ and $A = 2$, the algorithm converges in about 3–4 iterations and on the average 25 bits are transmitted to the fusion center. For $M = 6$, the fusion center has much more information about the source location at each iteration as compared to the $M = 5$ case, so the algorithm terminates faster as compared to the $M = 5$ case. Note that when A is large the fusion center has to select a large number of sensors using coarse information at the first iteration. Together with the use of distributed source coding, $A = 1$ yields the minimum number of bits transmitted to the fusion center until the end of the iterations.

VI. CONCLUSION

In this paper, we presented an iterative source localization method, where a coarse source location estimate is first obtained through the use of anchor sensors. Then, the posterior probability density function of the source location is approximated

[1]This assumption becomes more accurate with increasing M.

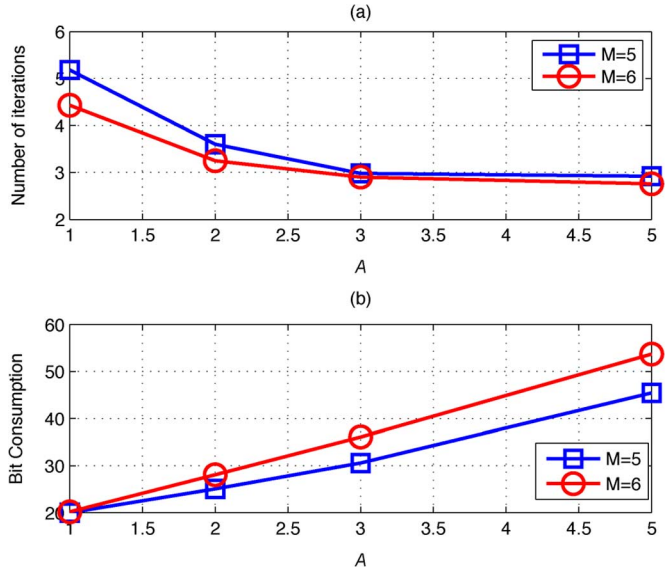

Fig. 7. (a) Average number of iterations until the termination of the algorithm. (b) Average total number of bits transmitted to the fusion center until the termination of the algorithm. ($\epsilon = 5$, 100 different trials.)

using a Monte Carlo method. We developed and compared two different sensor selection schemes for static source localization. The first scheme iteratively activates those non-anchor sensors that maximize the mutual information between source location and the quantized sensor measurements. In the second sensor selection scheme, at each iteration a number of non-anchor sensors are activated whose quantized data minimize the PCRLB. Simulation results show that, for large M, the MSE of the proposed iterative schemes gets close to the PCRLB for the case when all the sensor data are used, within a few iterations by selecting only the most informative sensors while significantly reducing the communication requirements. Simulation results show that the MI and PCRLB based sensor selection schemes achieve similar estimation performance and outperform the scheme that selects the sensors which are nearest to the estimated source location when M is small. PCRLB based sensor selection is better in terms of computational complexity. It has been shown that the computational complexity of MI based sensor selection increases exponentially with the number of activated sensors per iteration; while the computational complexity of PCRLB based sensor selection increases linearly with the number of activated sensors per iteration. The posterior pdf of the source location approximated based on the Monte Carlo method is further employed to compress the data of each activated sensor using distributed source coding techniques. As the uncertainty about the source location decreases, the conditional entropy of each activated sensor becomes small and their M-bit data can be compressed significantly.

In this work, we assumed that multi-bit sensor measurements are perfectly received at the fusion center. Future work will include channel fading and noise between sensors and the fusion center as well as defining the communication costs in terms of more specific path loss models. A theoretical framework can be developed to study the tradeoff between estimation performance in source localization and energy costs.

REFERENCES

[1] X. Sheng and Y. H. Hu, "Maximum likelihood multiple-source localization using acoustic energy measurements with wireless sensor networks," *IEEE Trans. Signal Process.*, vol. 53, no. 1, pp. 44–53, Jan. 2005.

[2] R. Niu and P. K. Varshney, "Target location estimation in sensor networks with quantized data," *IEEE Trans. Signal Process.*, vol. 54, no. 12, pp. 4519–4528, Dec. 2006.

[3] M. Nicoli, C. Morelli, and V. Rampa, "A jump Markov particle filter for localization of moving terminals in multi-path indoor scenarios," *IEEE Trans. Signal Process.*, vol. 56, no. 8, pp. 3801–3809, Aug. 2008.

[4] A. T. Ihler and J. W. Fisher, III, "Nonparametric belief propagation for self-localization of sensor networks," *IEEE J. Sel. Areas Commun.*, vol. 23, no. 4, pp. 809–819, Apr. 2005.

[5] H. Wang, K. Yao, G. Pottie, and D. Estrin, "Entropy-based sensor selection heuristic for target localization," presented at the 3rd Int. Symp. Information Processing in Sensor Networks (IPSN), Berkeley, CA, Apr. 2004.

[6] K. J. Hintz and E. S. McVey, "Multi-process constrained estimation," *IEEE Trans. Syst. Man Cybern.*, vol. 21, no. 1, pp. 237–244, Jan./Feb. 1991.

[7] F. Zhao, J. Shin, and J. Reich, "Information-driven dynamic sensor collaboration," *IEEE Signal Process. Mag.*, vol. 19, pp. 61–72, Mar. 2002.

[8] F. Zhao, J. Liu, J. Liu, L. Guibas, and J. Reich, "Collaborative signal and information processing: An information directed approach," *Proc. IEEE*, vol. 91, no. 8, pp. 1199–1209, Aug. 2003.

[9] C. M. Kreucher, K. D. Kastella, and A. O. Hero, "Sensor management using an active sensing approach," *Signal Process.*, vol. 85, no. 3, pp. 607–624, Mar. 2005.

[10] C. M. Kreucher, A. O. Hero, K. D. Kastella, and M. R. Morelande, "An information-based approach to sensor management in large dynamic networks," *Proc. IEEE*, vol. 95, no. 5, pp. 978–999, May 2007.

[11] J. L. Williams, J. W. Fisher, and A. S. Willsky, "Approximate dynamic programming for communication-constrained sensor network management," *IEEE Trans. Signal Process.*, vol. 55, no. 8, pp. 4300–4311, Aug. 2007.

[12] G. M. Hoffmann and C. J. Tomlin, "Mobile sensor network control using mutual information methods and particle filters," *IEEE Trans. Autom. Control*, vol. 55, no. 3, pp. 32–47, Jan. 2010.

[13] P. Tichavsky, C. H. Muravchik, and A. Nehorai, "Posterior Cramér–Rao bounds for discrete-time nonlinear filtering," *IEEE Trans. Signal Process.*, vol. 46, no. 5, pp. 1386–1396, May 1998.

[14] M. L. Hernandez, T. Kirubarajan, and Y. Bar-Shalom, "Multisensor resource deployment using posterior Cramér–Rao bounds," *IEEE Trans. Aerosp. Electron. Syst.*, vol. 40, no. 2, pp. 399–416, Apr. 2004.

[15] K. Punithakumar, T. Kirubarajan, and M. L. Hernandez, "Multisensor deployment using PCRLBs, incorporating sensor deployment and motion uncertainties," *IEEE Trans. Aerosp. Electron. Syst.*, vol. 42, no. 4, pp. 1474–1485, Oct. 2006.

[16] L. Zuo, R. Niu, and P. K. Varshney, "Posterior CRLB based sensor selection for target tracking in sensor networks," in *Proc. IEEE Int. Conf. Acoustics, Speech and Signal Processing*, Apr. 2007, vol. 2, pp. 1041–1044.

[17] L. Zuo, R. Niu, and P. K. Varshney, "A sensor selection approach for target tracking in sensor networks with quantized measurements," in *Proc. IEEE Int. Conf. Acoustics, Speech, Signal Processing*, Mar. 31–Apr. 4 2008, pp. 2521–2524, 2008.

[18] R. Tharmarasa, T. Kirubarajan, and M. L. Hernandez, "Large-scale optimal sensor array management for multitarget tracking," *IEEE Trans. Syst., Man, Cybern. C, Appl. Rev.*, vol. 37, no. 5, pp. 803–814, Sep. 2007.

[19] R. Tharmarasa, T. Kirubarajan, M. L. Hernandez, and A. Sinha, "PCRLB-based multisensor array management for multitarget tracking," *IEEE Trans. Aerosp. Electron. Syst.*, vol. 43, no. 2, pp. 539–555, Apr. 2007.

[20] M. Hurtado, T. Zhao, and A. Nehorai, "Adaptive polarized waveform design for target tracking based on sequential Bayesian inference," *IEEE Trans. Signal Process.*, vol. 56, no. 3, pp. 1120–1133, Mar. 2008.

[21] N. Brunel and J. P. Nadal, "Mutual information, Fisher information, and population coding," *Neural Comput.*, vol. 10, no. 7, pp. 1731–1757, Oct. 1998.

[22] P. M. Djuric, M. Vemula, and M. F. Bugallo, "Target tracking by particle filtering in binary sensor networks," *IEEE Trans. Signal Process.*, vol. 56, no. 6, pp. 2229–2238, Jun. 2006.

[23] A. Doucet and X. Wang, "Monte Carlo methods for signal processing, a review in the statistical signal processing context," *IEEE Signal Process. Mag.*, vol. 22, no. 6, pp. 152–170, Nov. 2005.
[24] J. Chou, D. Petrovic, and K. Ramchandran, "A distributed and adaptive signal processing approach to reducing energy consumption in sensor networks," in *Proc. IEEE 22nd Annu. Joint Conf. Computer Communications Societies*, Mar. 30–Apr. 3 2003, vol. 2, pp. 1054–1062.
[25] Z. Xiong, A. Liveris, and S. Cheng, "Distributed source coding for sensor networks," *IEEE Signal Process. Mag.*, vol. 21, pp. 80–94, Sep. 2004.
[26] H. L. Van Trees, *Detection, Estimation, and Modulation Theory, Part I*. New York: Wiley, 1968.
[27] D. S. Lee and N. K. K. Chia, "A particle algorithm for sequential Bayesian parameter estimation and model selection," *IEEE Trans. Signal Process.*, vol. 50, no. 2, pp. 326–336, Feb. 2002.
[28] D. Slepian and J. K. Wolf, "Noiseless encoding of correlated information sources," *IEEE Trans. Inf. Theory*, vol. IT-19, pp. 471–480, Jul. 1973.

Engin Maşazade (S'03) received the B.S. degree from the Electronics and Communications Engineering Department from Istanbul Technical University, Turkey, in 2003 and the M.S. degree from Sabanci University, Electronics Engineering Program, Istanbul, Turkey, in 2006. He is currently working towards the Ph.D. degree at the same university.

His research interests include bit error rate estimation and cross-layer design for multiband OFDM systems, distributed detection, estimation, localization for wireless sensor networks.

Mr. Maşazade has been awarded in 2008 for a research abroad support scheme from the Scientific and Technological Research Council of Turkey (TUBITAK) for his studies at Syracuse University under the supervision of Prof. P. K. Varshney.

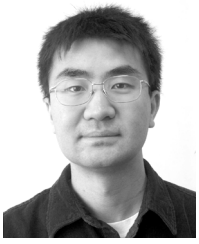

Ruixin Niu (M'04) received the B.S. degree from Xian Jiaotong University, Xian, China, in 1994, the M.S. degree from the Institute of Electronics, Chinese Academy of Sciences, Beijing, China, in 1997, and the Ph.D. degree from the University of Connecticut, Storrs, in 2001, all in electrical engineering.

He is currently a Research Assistant Professor with Syracuse University, Syracuse, NY. His research interests are in the areas of statistical signal processing and its applications, including detection, estimation, data fusion, sensor networks, communications, and image processing.

Dr. Niu received the Best Paper award at the Seventh International Conference on Information Fusion in 2004. He is the Associate Administrative Editor of the *Journal of Advances in Information Fusion*, and an Associate Editor of the *International Journal of Distributed Sensor Networks*.

Pramod K. Varshney (S'72–M'77–SM'82–F'97) was born in Allahabad, India, on July 1, 1952. He received the B.S. degree in electrical engineering and computer science (with highest honors) and the M.S. and Ph.D. degrees in electrical engineering from the University of Illinois at Urbana-Champaign in 1972, 1974, and 1976 respectively.

From 1972 to 1976, he held teaching and research assistantships at the University of Illinois. Since 1976, he has been with Syracuse University, Syracuse, NY, where he is currently a distinguished Professor of Electrical Engineering and Computer Science and the Director of CASE: Center for Advanced Systems and Engineering. He served as the Associate Chair of the department from 1993 to 1996. He is also an Adjunct Professor of Radiology at Upstate Medical University in Syracuse, NY. His current research interests are in distributed sensor networks and data fusion, detection and estimation theory, wireless communications, image processing, radar signal processing and remote sensing. He has published extensively. He is the author of *Distributed Detection and Data Fusion* (Springer-Verlag, 1997). He has served as a consultant to several major companies.

Dr. Varshney was a James Scholar, a Bronze Tablet Senior, and a Fellow while at the University of Illinois. He is a member of Tau Beta Pi and is the recipient of the 1981 ASEE Dow Outstanding Young Faculty Award. He was elected to the grade of Fellow of the IEEE in 1997 for his contributions in the area of distributed detection and data fusion. He was the guest editor of the special issue on data fusion of the PROCEEDINGS OF THE IEEE in January 1997. In 2000, he received the Third Millennium Medal from the IEEE and Chancellor's Citation for exceptional academic achievement at Syracuse University. He serves as a distinguished lecturer for the AES society of the IEEE. He is on the editorial board of *International Journal of Distributed Sensor Networks* and the *Journal of Advances in Information Fusion*. He was the President of International Society of Information Fusion during 2001.

Mehmet Keskinoz (M'98) received the M.S. and Ph.D. degrees from the Electrical and Computer Engineering Department, Carnegie Mellon University, Pittsburgh, PA, in 1997 and 2001, respectively.

In 2001, he joined the Electronics Engineering Program of Sabanci University, Istanbul, Turkey, where he is now an Associate Professor. His research interests include signal processing for wired and wireless communications, UWB communications, multi-band OFDM UWB systems, wireless mesh networks, magnetic and optical data storage systems, distributed detection and data fusion for wireless sensor networks, turbo and LDPC coding, synchronization, and digital watermarking.

Dr. Keskinoz was a recipient of Turkish NSF Research grant on distributed detection in wireless sensor networks and Career Award on wireless mesh networks in August 2005. He is a Co-Guest Editor of the *IEEE Communications Magazine* January 2009 Special Issue on Advances in Signal Processing for Wireless and Wired Communications. He is a member of the IEEE Communication Society, theIEEE Signal Processing Society, and the Optical Society of America.